JET–P(97)33

Plasma-edge Gradients in L-mode and ELM-free H-mode JET Plasmas

P Breger, C Flewin[1], K-D Zastrow, S J Davies, N C Hawkes[2], R W T König, Z A Pietrzyk[3], L Porte[4], D D R Summers and M G von Hellermann

JET Joint Undertaking, Abingdon, Oxfordshire, OX14 3EA, UK.
[1]University College London, Gower Street, Bloomsbury, London WC1E 6BT, UK.
[2]UKAEA Fusion/Euratom Association, Culham, Abingdon, Oxon, Ox14 3DB, UK.
[3]CRPP, Lusanne, Switzerland.
[4]UCLA, Department of Elec.Eng., Los Angeles, CA 90095-1597, USA.

Preprint of a paper to be submitted for publication in
Plasma Physics and Controlled Fusion

October 1997

ABSTRACT

Experimental plasma-edge gradients of electron and ion densities and temperatures in JET during the ELM-free H-mode are examined for the presence of the transport barrier region inside the magnetic separatrix. High spatial resolution data in electron density is available from a Li-beam diagnostic, and in electron temperature from an ECE diagnostic. A reciprocating probe provides highly spatially resolved electron density and temperature data in the SOL outside the separatrix. Ion temperatures and densities are measured using an edge charge-exchange diagnostic. A comparison of the electron density gradients in L-mode and H-mode is made. The behaviour of observed widths and gradients of this edge region are compared with each other and with theoretical expectations. The electron temperature barrier width (3-4cm) is about twice that of electron density. By suitable parameterisation of the edge data, an electron pressure gradient can be estimated. This is seen to rise during the ELM-free phase to reach about half the marginal pressure gradient expected from ballooning stability before the first ELM. Subsequent ELMs are seen to occur on a pressure gradient contour given by either a constant barrier width model or a ballooning mode envelope model of width $(\rho/a)^{2/3}r$, *the normalised ion Larmor radius.*

1. INTRODUCTION

The transition from L- to H mode confinement is accompanied by the formation of a narrow region of reduced energy and particle transport inside the plasma boundary as given by the separatrix (Bak *et al.* 1996, Itoh and Itoh 1988). Large temperature and density gradients develop within a transport barrier region of width Δ inside the magnetic separatrix, with a low density and temperature plasma in the scrape-off layer outside the separatrix. The ion orbit loss model (Shaing and Crume 1989) predicts Δ to be of similar magnitude as the ion poloidal gyroradius, scaling with ion temperature and poloidal field. Allowing for squeezed ion banana widths (Shaing 1992), scalings with ion temperature only occur. An alternative viewpoint is that the width is related to the penetration length of neutrals originating from recycled plasma particles or gas puffing, and scalings of Δ with the effective ionisation length (by collisional ionisation and charge-exchange) are expected. Furthermore, in the H-mode regime, the edge pressure gradient profile is limited by the ballooning mode stability, with the width of the barrier region given by the mode envelope. A recent higher order edge ballooning theory (Connor and Wilson 1997) predicts Δ to scale with $(\rho/a)^{2/3}r$, the ion Larmor radius normalised to the plasma minor radius. This latter model was found to compare well with the pedestal pressure attained in ELMy H-mode discharges at JET prior to the onset of type I ELMs (Lingertat 1997).

Experimental verification of the scaling behaviour of the barrier width, the pedestal density and temperature, as well as the pressure gradient limits achieved before onset of loss of confinement (e.g. type I ELMs) require detailed measurement of edge temperature and density with high spatial resolution and positional accuracy. This paper presents various high resolution edge measurements at JET during the ELM-free H-mode, and examines suitable means of parameterisation of these to investigate scaling behaviours. The electron density data is presented in section 3, electron temperature data in section 4 and ion parameters in section 5. By parameterisation of the electron edge data using a tanh fit, profiles in electron pressure gradient can be estimated (section 6) and compared with ballooning mode theory predictions.

2. PARAMETERISATION OF EDGE PROFILES

In order to characterise the plasma edge, a parameterisation of edge gradient, pedestal value and barrier width using three different algorithms was developed and compared :

- bi-linear fit of core gradient and edge gradient
- non-linear fit of edge profile deviation from linear core gradient
- a composite fit of the core and edge profile based on a tanh function (Groebner and Carlstrom 1996)

$$T(r) = A \cdot \tanh\left(\frac{r_{mid} - r}{\delta}\right) + B + \frac{dT}{dr} \cdot (r_{mid} - r - \delta) \cdot \Theta(r_{mid} - r - \delta),$$

where $\Theta(x)$ is the Heaviside step function = 1 for x≥0 , and =0 for x<0. The width parameter δ is related to the barrier width by $\delta = 0.5\Delta$. An example of the bi-linear fit and the tanh fit are shown for a typical electron temperature measurement in figure 1. Comparisons of the barrier widths obtained from the three methods for ELM-free hot-ion H-mode plasmas at JET showed good agreement, and an investigation of the behaviour of the width using the bi-linear fit was undertaken. To calculate a pressure and pressure gradient profile, however, the tanh fit was used.

3. THE ELECTRON DENSITY PROFILE

The edge electron density profile is measured using a 60 keV Li-beam and a reciprocating probe (RCP) near the stagnation point at the top of the vessel at the same poloidal coordinate. Direct

data comparison without the requirement of magnetic surface mapping is possible. Density profiles are obtained by de-convolving the Li-beam emission profile over a length of 17 cm with resolution of 0.7cm using an algorithm based on evaluation of the beam excitation and ionisation balance (Pietrzyk, Breger and Summers 1993). This requires beam current, edge temperature profile data and impurity concentration as input. To facilitate a consistent analysis a three region model for ion and electron temperature profiles in- and outside the separatrix based on ECE, CXRS, reciprocating probe and Lidar measurements has been used (table 1).

	L-mode plasma	**H-mode plasma**
Core region	LIDAR profile	LIDAR profile
Barrier region	Linear rise in T to join SOL/core over a region of width 5–7cm	Linear rise in T to join SOL/core over a region of width 5–7cm
SOL region	At sep. = 40eV, expon. fall-off at 15cm to outside	At sep. = 70eV, expon. fall-off at 5cm in ELM-free and 15cm in ELMy plasmas

Table 1 : Temperature model used for de-convolution of Li-beam emission data, using $T_e=T_i$

Variation of input parameters within their experimental uncertainties indicates that the resultant $N_e(r)$ profile has an estimated error of <20% at peak density. A constant concentration of 3% C is used in the code to match the bulk Z_{eff} of ~1.8-2.0 as measured by the core charge-exchange diagnostic system.

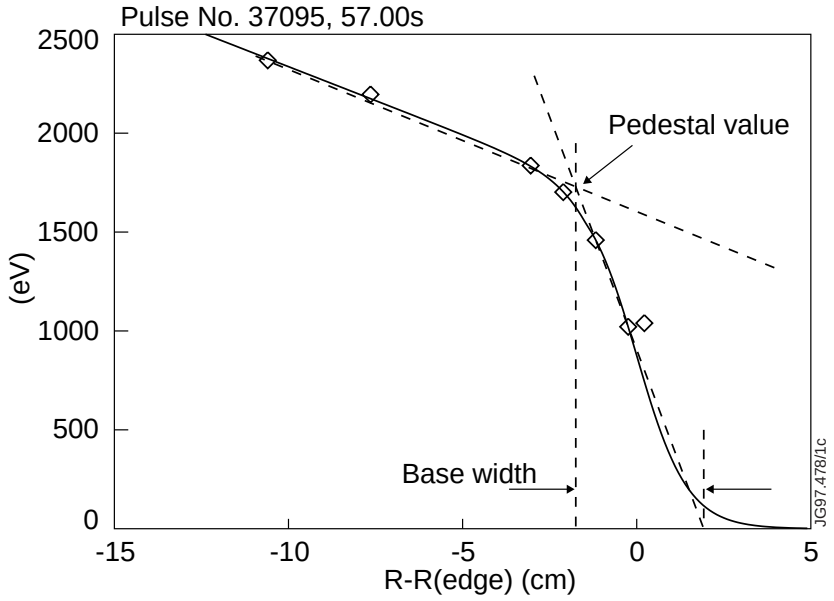

Fig. 1: Definition of edge gradient measures, illustrated for the example of an ECE temperature profile.

3.1 COMPARISON OF EDGE DENSITY DATA FROM DIFFERENT DIAGNOSTICS

The density profile of the Li-beam is compared to RCP results in fig. 2 (absolute position errors ~ ±2cm and ±1cm respectively) , and with core Lidar data (corrected in absolute value using FIR interferometer results) in fig. 3.

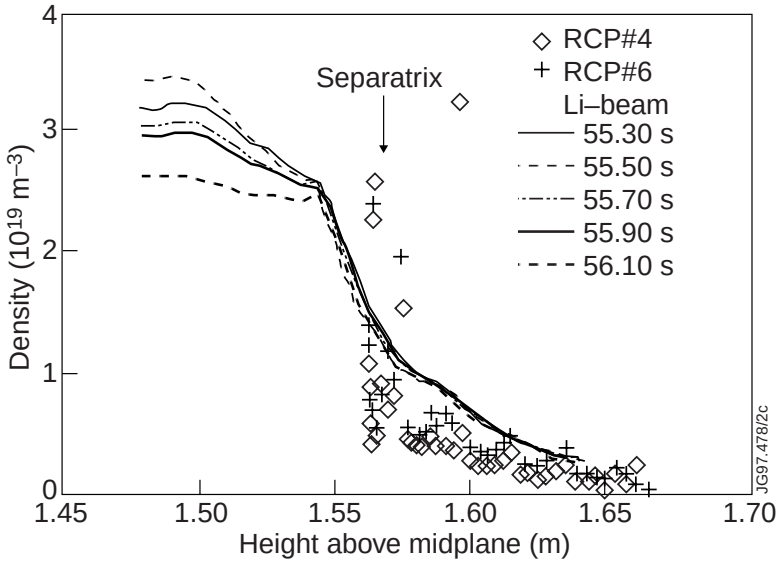

Fig. 2: Comparison of Li-beam electron density profiles with RCP profile data. The reciprocating probe scan covered four exposure periods of the Li-beam diagnostic from 55.3 to 56.1s.

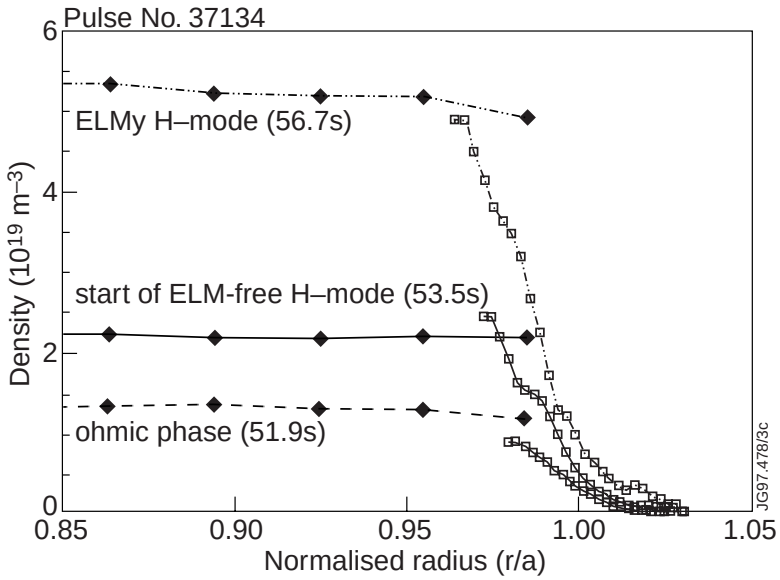

Fig. 3: Comparison of Li-beam electron density profiles (open symbols) with core density data (solid symbols) for three different phases of the discharge

For the latter comparison the EFIT magnetic equilibrium code is used to transform the top edge data to midplane radii. The error in the resulting midplane position is estimated to be of order ±1 cm. The densities at the separatrix are found to be of order 15% of the line average core plasma density

(fig. 4), with the major part of the measured electron density gradient lying inside the magnetic separatrix in the transport barrier region.

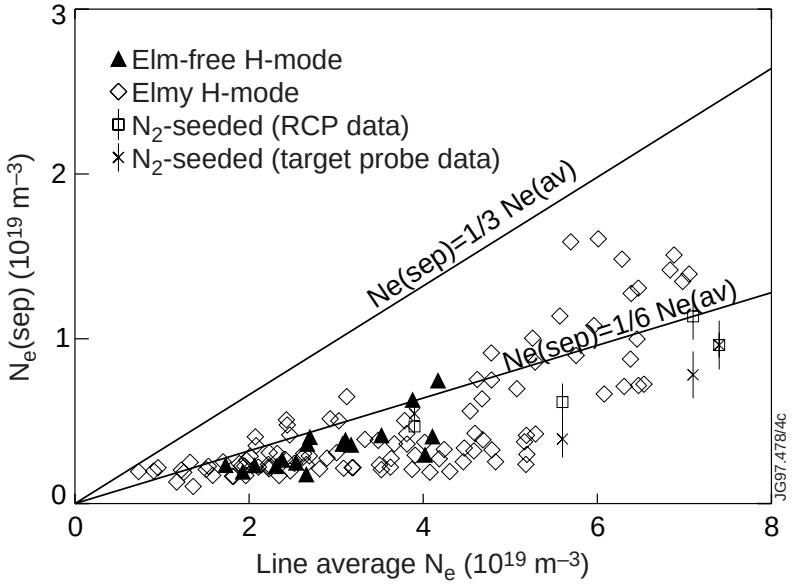

Fig. 4: Comparison of separatrix densities as function of line-average density during H-mode. Reciprocating probe and target probe results from N_2-seeded plasmas are shown for comparison

Whereas the Li-beam data for ELMy discharges is averaged over ELMs, analysis of probe edge data is done at better time resolution between ELMs, and yields a similar result. The latter shows that the ratio $N_{e\text{-}sep}/N_{e\text{-}av}$ is larger for heavier gas puffing rates and higher ELM frequency, the ELM frequency being strongly increased by the gas puff rate for a given configuration.

3.2 THE L- AND H-MODE EDGE

To study the differences of electron density gradients in L and H-modes, data was obtained for a series of similar discharges with a long outer limiter period followed by a neutral beam heated Hot-ion H-mode phase (X-point plasma). Comparing the density profiles between limiter and H-mode phase, a strong steepening of the electron density at the transition into H-mode is observed (figure 5). Whilst the density inside the separatrix rises with increase in central density, the density outside the separatrix is little affected. An exponential density fall-off length is fitted over short sections of the profile around the separatrix. The fall-off length mapped onto the midplane plasma radius is shortest during the ELM-free H-mode phase with a value of 0.8 cm in the midplane. The plasma performance as given by the enhancement H-factor over the ‘89 L-mode energy confinement time scaling is found to correlate with the fall-off length (figure 6). A

small density gradient width is seen to be a pre-requisite, but not the only factor responsible for good confinement. The ELM-free plasma state is seen to develop for the steepest density edge.

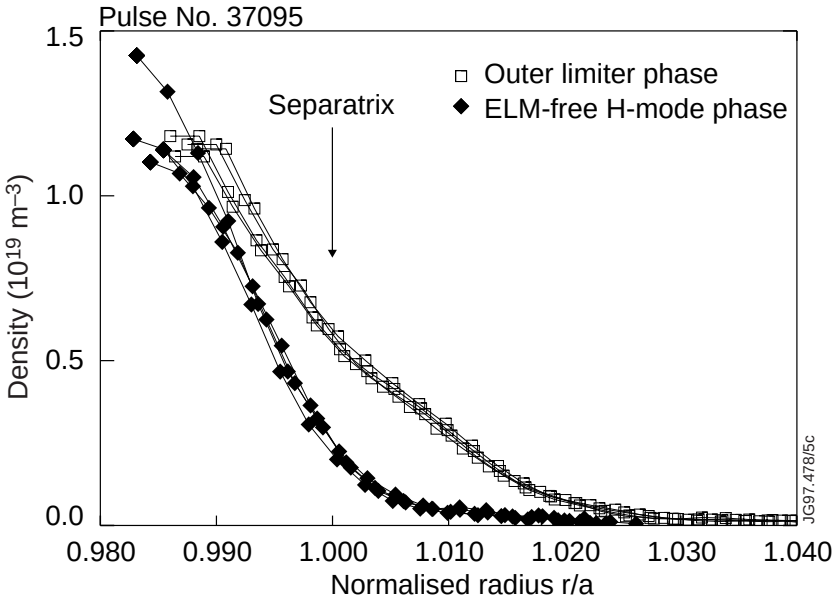

Fig.5 : Comparison of edge density profiles from an outer limiter plasma and the subsequent hot-ion H-mode (#37095).

Investigation of scaling behaviour of the fall-off length with respect to edge power loss, plasma energy, temperature and density, and connection length show no clear dependence. However, some dependence is observed between the measured fall-off length and the configuration-dependent local B_{pol} induced by plasma current and shaping coils, although the small variation in local B_{pol} in the available data makes determination of a scaling law impossible.

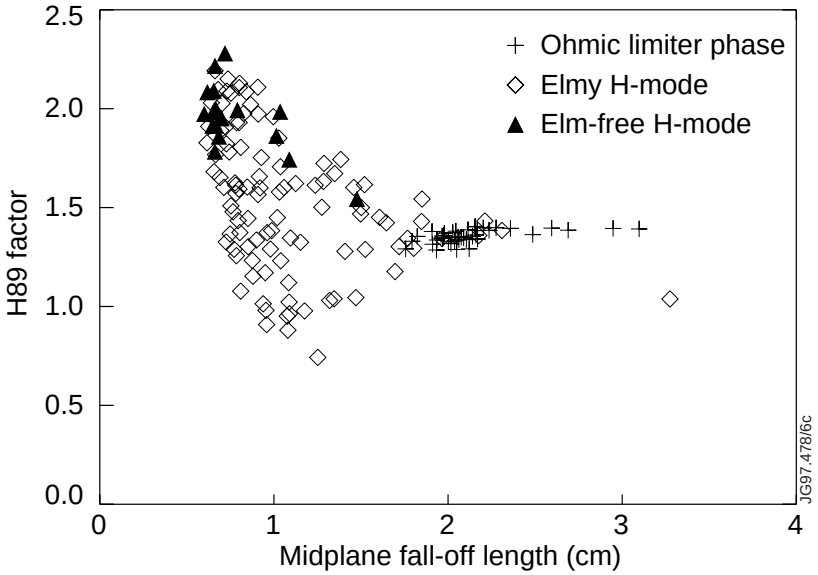

Fig. 6 : H-mode performance as function of density fall-off length (converted to cm at plasma midplane).

4. THE ELECTRON TEMPERATURE PROFILE

The electron temperature profile within the last closed flux surface is measured using a midplane ECE diagnostic. Due to large temperature gradients at JET and the presence of a significant fraction of relativistic electrons the spatial resolution is limited to about 1.5 cm (Porte, Bartlett Conway and Smeulders 1997). Measurements are taken at 250 kHz. Analysis of electron temperature profiles for a dataset of 180 ELM-free H-mode cases shows (figs. 7-9) :

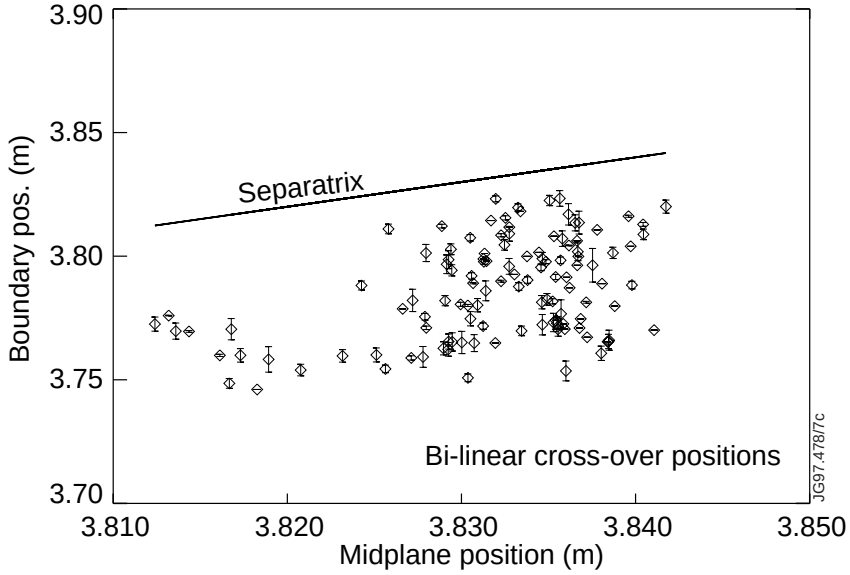

Fig. 7: Positioning of temperature barrier relative to EFIT separatrix position

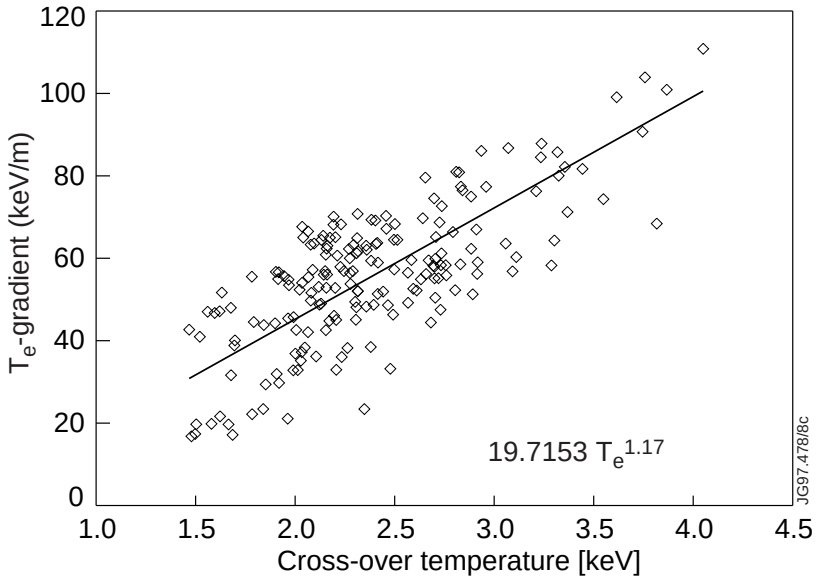

Fig. 8: Scaling of temperature gradient with pedestal temperature

- the pedestal temperature (cross-over between core and edge linear fits) rises during the entire ELM-free H-mode from about 2.5 to 3 keV ;

- the edge temperature gradient builds up at the start of the first hot-ion ELM-free H-mode phase in about 0.2-0.3 s ;

- the barrier width is nearly constant at 3-4 cm in this first ELM-free phase, compared to 5-8 cm between ELMs (Lingertat 1997);

- the cross-over point of the core and edge gradients lies at a position well inside the separatrix position given by EFIT and defines a pedestal temperature point, the edge gradient intercepts zero temperature around the separatrix position;

- a scaling law for the edge gradient, consistent with the time varying behaviour, is found to be $\nabla T_e \sim T_e^{1.16\pm0.09} \cdot I_p^{0.01}$ and $\Delta \sim T_e^{-0.16\pm0.09}$, hence no plasma current dependence is seen in the data from plasmas at 1.2 and 2.5 MA.

It should be noted that the scaling laws derived from the time variant data contain the correct physical inverse relation between linear gradient and width. A regression analysis of data towards the end of the ELM-free H-mode only was found to violate this basic relation, as it was dominated by noise in the experimental data rather than the T_e dependence.

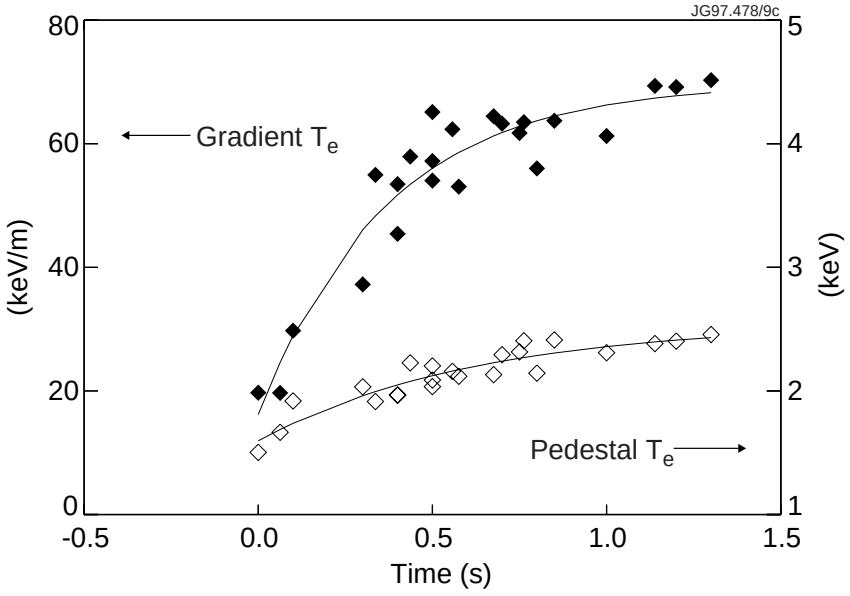

Fig. 9: Edge temperature (open symbol) and temperature gradient (solid symbol) evolution during ELM-free H-mode

5. THE ION TEMPERATURE AND DENSITY PROFILE

Ion temperatures and densities in the edge are measured using an active midplane charge-exchange diagnostic, monitoring the n=8-7 transition in C^{5+} . Data obtained for plasmas with currents from 1MA to 2.8 MA, and fields of 2.5T to 2.9 T has 1 cm radial resolution.

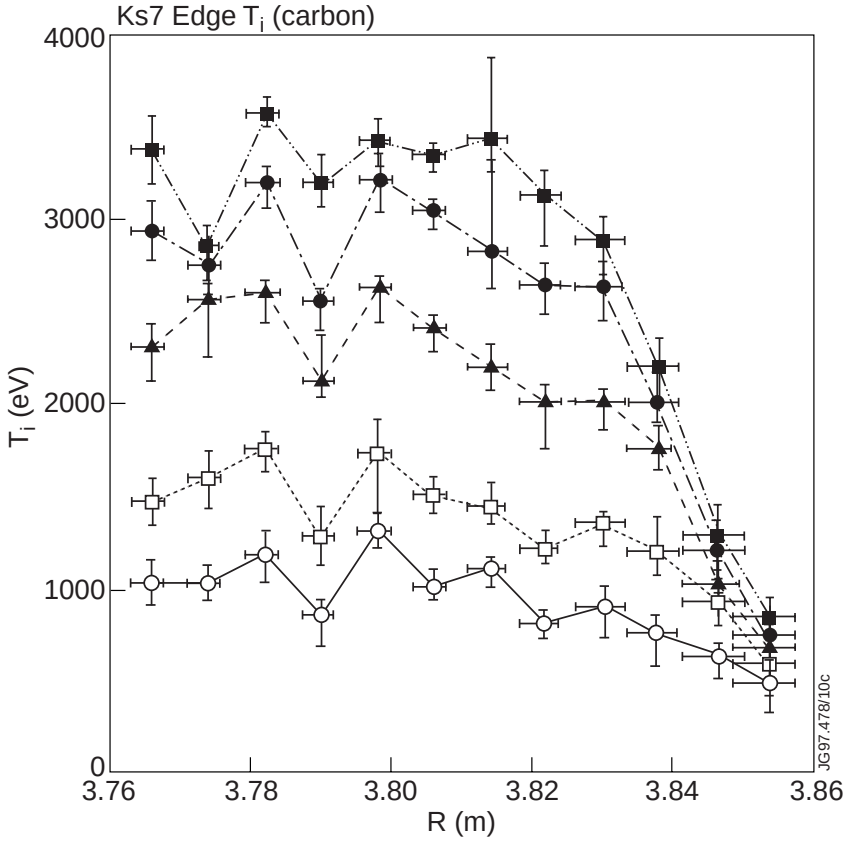

Fig. 10:Ion temperature profile evolution before onset (lower 2 traces) and during ELM-free phase (upper 3 traces)

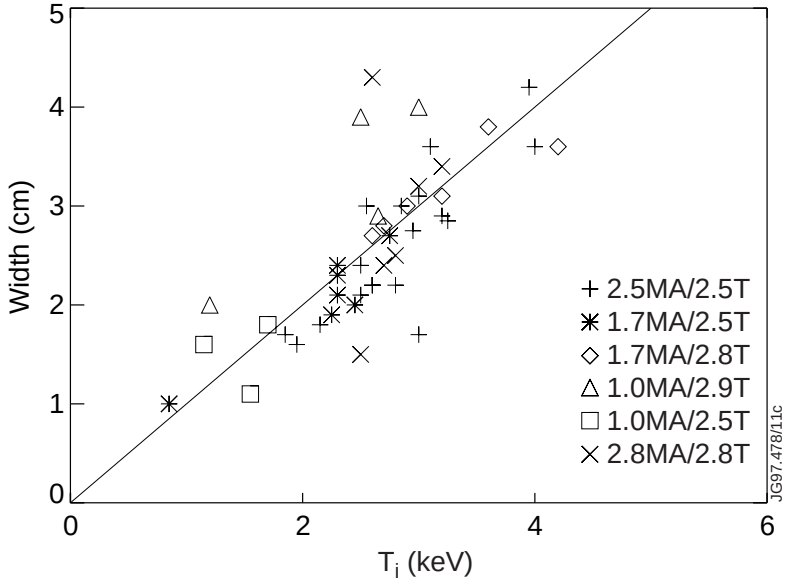

Fig. 11: Ion temperature barrier width as function of ion temperature (using a bi-linear profile fit).

Examination of the temperature-time traces shows that successive chords cease to increase with the increasing pedestal value and begin to maintain a constant maximum gradient between neighbouring chords during the ELM-free period. This suggests that the barrier width is varying linearly with the temperature, as seen in the evolution of the temperature profiles (figure 10). Using the bi-linear model for ELM-free H-mode discharges of varying plasma current, the edge gradient is not seen to scale with toroidal plasma current, giving a constant barrier gradient of 1.0±0.1 keV per cm (figure 11). However, the size of the measured T_i barrier width is of order 3 to 4 cm similar to the T_e barrier.

Impurity ion density profiles were also obtained from the data. Whereas the absolute ion density is critically dependent on absolute channel calibration, the profile shape development can be measured with good accuracy. It is found that the ion density profile barrier widths are nearly always the same as those for the temperature.

6. THE ELECTRON PRESSURE PROFILE $P_E(R)$ AND BALLOONING LIMIT

To infer the electron pressure profile $P_e(r)$ from N_e and T_e data, both profiles need to be mapped onto the same grid with an accuracy better than the typical gradient scale length. In the following discussion, the ELM-free hot-ion H-mode plasma of pulse #37095 (2.5MA, 2.6T) discussed

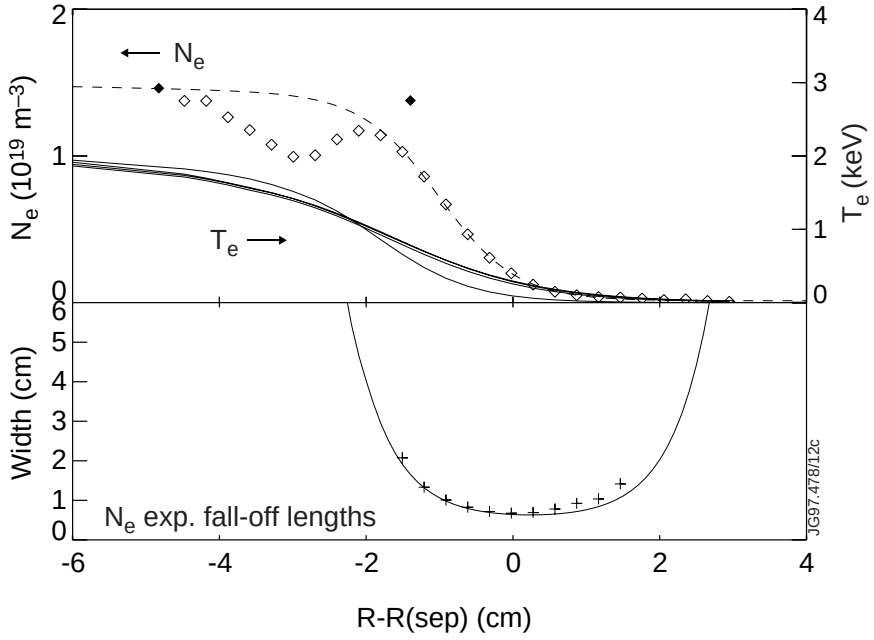

Fig. 12 : Combining electron density and temperature data to a pressure profile: a) tanh fit to density (open symbol = Li-beam, solid symbol = Lidar) and temperature profile (ECE) in midplane coordinates, b) the corresponding 1/e fall-off lengths (+ = exponential fit to N_e, line = tanh fit to N_e)

above is analysed. The electron density $N_e(r)$ is mapped to a midplane radius using EFIT equilibria, and its absolute position is estimated to be known to 1cm. The linear fit of the edge temperature $T_e(r)$ (inside the separatrix) is extrapolated to zero temperature, this point is then identified as

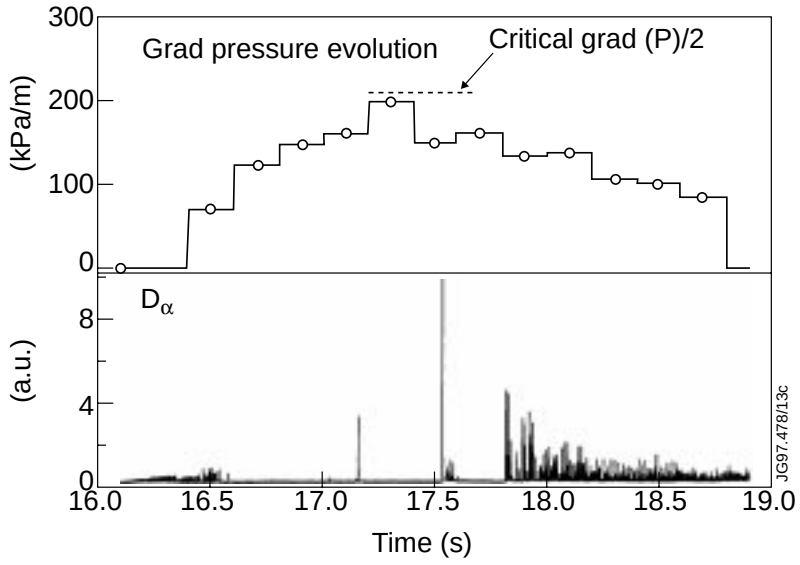

Fig. 13 : Computed electron pressure profile gradient (assuming coincident max. gradients) and $D\alpha$ emission. The estimate of the marginal ballooning pressure gradient for electrons is given assuming $\nabla P_e = \nabla P_i$. The ∇P increases during ELM-free phase until ELMs occur.

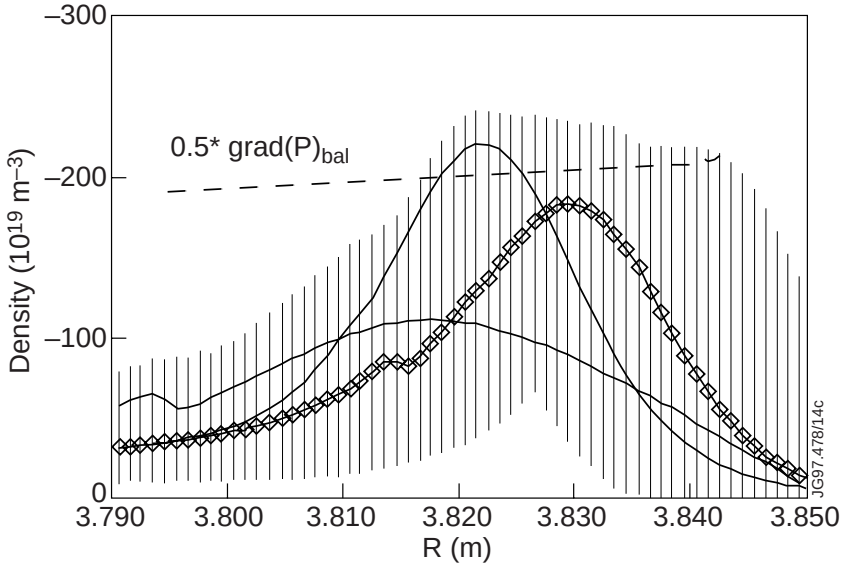

Fig. 14 : Measured electron pressure gradient (symbols) at time 57.3s before occurence of ELM . The shaded region corresponds to error range due to absolute position errors of 1cm in density and 2cm in temperature profiles, with solid curves for cases of +1cm,-2cm and -1cm,+2cm. The broken line corresponds to half of the estimated marginal ballooning pressure gradient profile.

the separatrix location, giving an error of about 2cm in position. A composite tanh function fit is then applied to both profiles (figure 12a). The fall-off length δ of the tanh fit in the density data compares well with piecewise exponential fall-off lengths fitted to the density profile (figure 12b). The width of the T_e edge gradient is determined using the three methods discussed in section 1, and yield $\Delta T_e = 3.8 \pm 0.4$ cm. The electron density edge width $\Delta N_e = 2\delta = 2 \pm 0.2$ cm is half the electron temperature edge width. The calculated $\nabla P_e(r)$ is compared in figure 13 with the estimates of the critical $\nabla P_{crit}(r)/2$ for ballooning modes. Also shown is the $D\alpha$-signal indicating the different phases of the H-mode development. The pressure gradient is seen to build up during the ELM-free phases and to collapse at the occurence of ELMs. In figure 14 the electron pressure gradient profile before the ELM at 57.5s is compared with half the computed marginal ballooning pressure gradient. The shaded region indicates the range of pressure gradients resulting from the 1cm and 2cm errors in position of density and temperature profile fit.

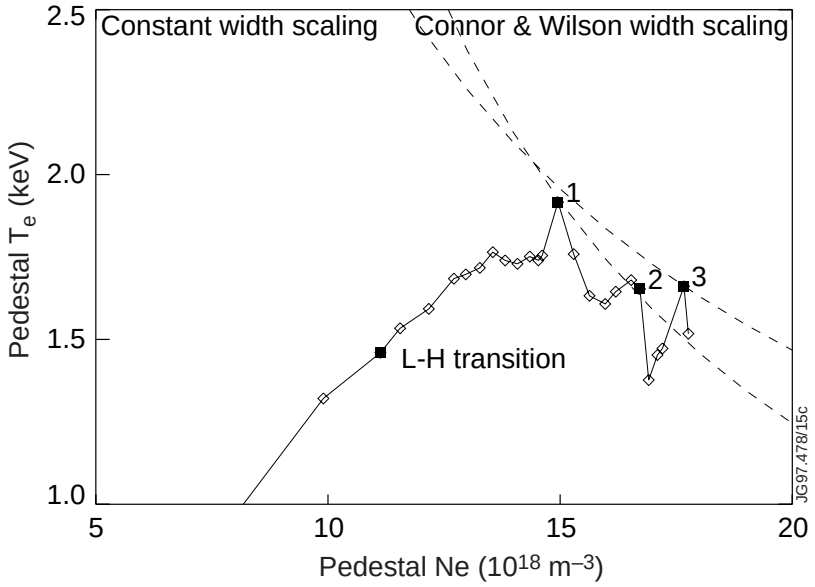

Fig. 15 : Trajectory of pedestal pressure evolution for #37095. The L-H transition is followed by a hot-ion ELM-free H-mode, which ends with ELM 1, followed by further type I ELM events 2 and 3. The broken curves correspond to constant pressure gradient contours.

Since the profile shape is well parameterised by a tanh shape, the pedestal temperature and density are linked to the pressure gradient by a simple relation

$$\nabla P_e = \frac{1}{2} T_e^{ped} N_e^{ped} \left(\frac{1}{\Delta_N} + \frac{1}{\Delta_T} \right) = \frac{3}{4} \frac{T_e^{ped} N_e^{ped}}{\Delta_N}$$

This provides the basis for using pedestal values to obtain a stability diagram (Kaufmann *et al.* 1996, Lingertat 1997, Osborne *et al.* 1996). Such an edge pedestal diagram for #37095 is

shown in figure 15, together with the key events of the L-H transition, followed by the first, second and third ELM. The L-H transition is followed by an ELM-free phase during which the pedestal pressure rises until the ballooning limit is reached. A critical pressure gradient contour is in the case of constant barrier width a constant pressure curve in the T_e-N_e diagram. Similar critical pressure gradient curves can be drawn for other $\Delta = f(T_e, N_e)$ relationships. Two contours of constant pressure gradient are shown for comparison: one for constant barrier width and one for the recent higher order edge ballooning theory of Connor and Wilson 1997 where $\Delta \sim (\rho/a)^{2/3} r$. Subsequent ELMs occur at roughly the same pressure gradient contour. Within experimental accuracy both models for an upper limit are consistent with the data. Further work is needed to obtain edge ion pressure gradients with sufficient accuracy to compare the total plasma pressure before type I ELMs with different scaling laws.

7. CONCLUSIONS

In order to obtain an experimental characterisation of the electron plasma edge gradients in the ELM-free H-mode phase, detailed electron density profiles have been obtained with the Li-beam diagnostic, which compare well with the data from RCP and Lidar. In H-mode the edge is seen to steepen inside the magnetic separatrix, showing the formation of a transport barrier.

The ion edge gradients have been investigated using a edge charge-exchange diagnostic. The ion temperature gradient exhibits a constant gradient of 1 keV/cm for a range of plasma currents, which does not fit the poloidal ion gyroradius model. The ion density gradient is of the same width or wider than the ion temperature gradient. The electron temperature gradient as obtained from ECE measurement builds up during 0.2 to 0.3 s of the ELM-free period. The electron temperature barrier width exhibits a behaviour in contradiction to ion gyro-radius models, with a constant barrier width of approx. 3-4 cm in ELM-free H-mode discharges, rather than the $\sqrt{T_e}$ dependence. The electron temperature barrier width is about twice the electron density barrier width.

Edge profile characterisation using a tanh fit allows electron pressure gradient profiles to be calculated from noisy experimental data. The resultant electron pressure gradient reached before a type I ELM event is of order 1/2 of the critical ballooning mode gradient for total pressure, subsequent ELM events reach a similar pressure gradient.

ACKNOWLEDGEMENTS

We wish to thank the Swiss National Science Foundation and UK DTI for partially funding this work.

REFERENCES

Bak P. *et al.* (1996) Nuclear Fusion **36**, 3, p 321

Connor J.W. and Wilson H.R. (1997) UKAEA Fusion Plasma Physics Note 97/4.1

Groebner R. and Carlstrom T. (1996) " Parameterization of Edge Profiles for H-mode Studies", Bulletin of the American Physical Society, APS Conference, Denver, Colorado

Itoh S-I. and Itoh K. (1988) Phys. Rev. Letters **60**, 22, p 2276

Kaufmann M.,Schweinzer J.,Albrecht M. et al. (1996), "Overview of ASDEX Upgrade Results" , IAEA-CN-64/O2-5, 16th IAEA Fusion Energy Conference, Montreal, Canada

Lingertat J. (1997) ,"The ELM operational window and power deposition in JET", Or-O1, 24th EPS conference on Controlled Fusion and Plasma Physics, Berchtesgaden, Germany

Osborne T et al. (1996), "ELM Studies on DIII-D", Bulletin of the American Physical Society, APS Conference, Denver, Colorado

Pietrzyk Z.A., Breger P., Summers D.D. (1993) Plasma Phys. Control. Fusion **35**, p 1725

Porte L., Bartlett D.V., Conway G., Smeulders P. (1997) ,Proc. of the 10th Intl. Workshop on ECE and ECRH, Ameland, Netherlands

Shaing K.C. and Crume E.C. (1989) Phys. Rev. Letters **63**, 21, p 2369

Shaing K.C. (1992) Phys. Fluids **B4**, 2, p 290